Phenomenological Analysis of the Martensitic Transformation in Y-PSZ

M. Hayakawa and M. Oka

Department of Mechanical Engineering, Tottori University, Koyama, Tottori 680, Japan

Abstract

The phenomenological theory of martensitic transformation was applied to the herringbone tetragonal to monoclinic phase transformation in Y-PSZ. Input data for the calculation were chosen from previously obtained data on an arc-melted ZrO_2–2mol%Y_2O_3 alloy. The observed striations along a $\{101\}_m$ plane in the m-plates were assumed to be the trace of lattice invariant shear, *i.e.*, twinning or slip on the plane. Among twenty solutions, four were found to be consistent with the experimentally observed habit planes and orientation relations. Although these four solutions were not crystallographically equivalent, they were all similar and predicted the same $(\bar{7}02)_m$ habit planes. Calculation was also made for the case where the parent was a single variant tetragonal lattice. Two extra solutions with $(\bar{11}02)_m$ and $(\bar{5}02)_m$ habit were predicted in addition to the same four solutions predicted for the herringbone tetragonal parent.

1. Introduction

The tetragonal to monoclinic phase transformation in zirconia and PSZ(Partially Stabilized Zirconia) is well known to be martensitic[1,2]. The crystallography of martensitic transformation is best studied by the phenomenological theory of martensitic transformation[3,4], and a few applications to zirconia systems can be found in the literature[5-8]. In these studies, however, evaluation of the results was difficult mainly because of the lack of detailed experimental data to compare with. In our recent study using coarse grained specimens prepared by arc-melting, sufficient data were accumulated for a detailed phenomenological analysis[9,10]. Although the results has been partly reported elsewhere[11], a more comprehensive description of the procedure and results is aimed here. In addition, an analysis is made for the case where the parent lattice is single variant tetragonal.

2. Summary of crystallographic data

Table 1 summarizes crystallographic data obtained in previous experimental works[9,10]. Individual items are briefly explained in the following.

2.1 Specimens

The specimens were prepared by plasma-arc-melting * of sintered ZrO_2 -2mol%Y_2O_3 † pellets on a water cooled copper hearth. The lattice parameters were measured on mixed phase powders prepared by pulverizing a sintered body. Arc-melted specimens contained grains of ~1mm and were fully tetragonal at room temperature. Since the t-phase persisted even at 77K, the m-phase was induced by aging at 523K in air for several hours.

2.2 Structure of the parent phase

Figure 1 shows an electron micrograph of a few m-plates produced in the parent phase. The parent t-phase exhibits a typical herringbone structure comprising two types of parallel bands with $\{101\}_t$ twins, as schematically dipicted in Fig. 2. When three mutually perpendicular t- variants are denoted by x, y, and z, one type of band comprised $(101)_t$ or $(\bar{1}01)_t$ twins of x and z variants and the other $(011)_t$ or $(0\bar{1}1)_t$ twins of y and z variants. The band boundaries are parallel to a $(110)_t$ or $(\bar{1}10)_t$ type plane. In order that the overall shear strain of the c-t transformation be minimized,

* Model: NMB.PLASMA-300AW, Nippon Miniature Bearing Co., LTD., Tokyo, Japan

† TZ-2Y powder: Y_2O_3 3.68wt%, oxide inpurity 0.038wt%, Tosoh Co., Tokyo, Japan

Table 1. List of experimental data

Specimen	Arc-melted $ZrO_2 - 2mol\%Y_2O_3$	
Lattice parameters	$a_t = 0.51003$ nm	$a_m = 0.51570$ nm
	$c_t = 0.51866$	$b_m = 0.51909$
	$c/a = 1.017$	$c_m = 0.53251$
		$\beta = 98.61$ deg
Parent phase structure	Stack of $(101)_t$ twins with x var./z var.$= 2/1$	
Lattice correspondences	$ABC, AC\bar{B}, BCA, \bar{B}AC, CAB, C\bar{B}A$	
Lattice invariant shear	$\{101\} < 10\bar{1} >_m$ slip	
	$\{101\} < 010 >_m$ slip	
	$\{101\}_m$ twin	
Observed orientaion relation	$(100)_m//\{100\}_t$,	
	$[001]_m// < 001 >_t$	
Observed habit plane	$\sim (\bar{3}01)_m$	

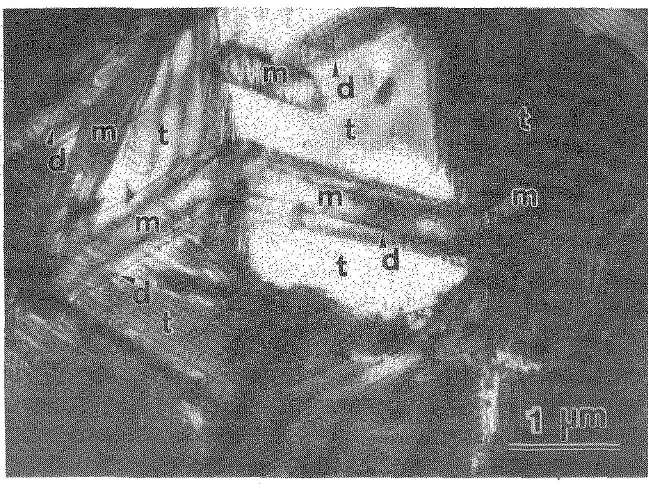

Fig. 1. Electron micrograph of the t-phase herringbone structure and m-plate.

the volume fractions of the three variant must be equal. This condition requires that the twin ratio in each band, *i.e.* x/z and y/z, is equal to 2. Although deviations were locally observed, the above described condition appeared fulfilled on an average.

The m-phase forms in a planar shape in this structure. It was observed that these m-plates sometimes extended straight across several bands but they were usually arrested at a band boundary, often emitting another plate into either side of band(see Fig. 1). These observations suggest that an m-plate fulfills an invariant plane strain condition, which is the basis of the phenomenological theory, in each band separately. Since all bands are crystallographically equivalent, we arbitrarily choose a band comprising $(101)_t$ twins of x-z variants with the ideal twin ratio of 2, *i.e.*, A band in Fig. 2, as a parent structure.

2.3 Lattice correspondence

Since a unit cell size is similar for both the t- and m-lattices, mutual correspondence between the principal axes is obvious. Because a and b axes are equivalent for a tetragonal lattice, three nonequivalent LCs(lattice correspondences) arise between a single variant t-lattice and the m-lattice. Namely, denoting the principal axes of the m-lattice by A, B, and C, the lattice correspondence with the tetragonal a b c axes maybe expressed by ABC, BCA, and CAB. In the present case, however, since the a, b, and c axis directions of the z-variant have different symmetry owing to the presence of the $(101)_t$ twins, these three axes must be distinguished. Thus the following six nonequivalent LCs arise, *i.e.*, ABC, $AC\bar{B}$, BCA, $\bar{B}AC$, CAB and $C\bar{B}A$. (The minus signs are attached so that the

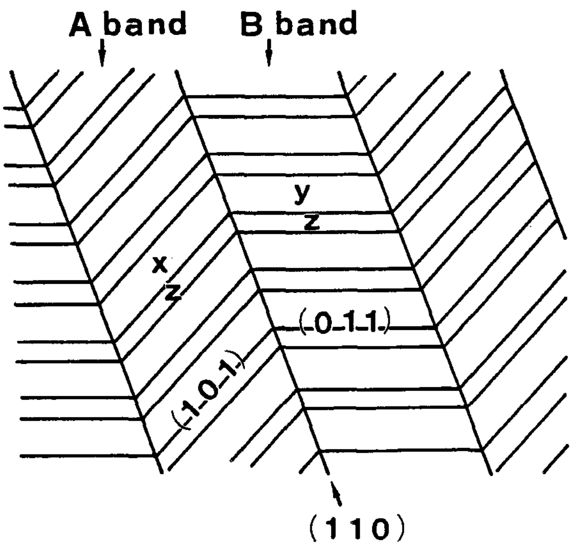

Fig. 2. Schematic representation of the t-phase herringbone structure.

axes conform with a right handed coordinate system). Since we do not have any reason to assume any of these six LCs are preferred in practice, calculation will be made for all six nonequivalent LCs.

2.4 Lattice invariant shear systems

The phenomenological theory assumes that a martensite plate fulfills an invariant plane strain condition with respect to the matrix. Since the lattice strain from the parent to the product lattice is not normally an invariant plane strain, an additional strain called lattice invariant strain(LIS) by slip or twinning is assumed to take place so that the total strain becomes an invariant plane strain. When the LIS system is not known, plausible LIS systems are assumed for calculation. When the number of assumed LIS systems is large, however, a large number of solutions arise accordingly and thus it becomes difficult to make sensible comparisons with experimental observation. Fortunately in the present specimen, fine striations, which were similar to the LIS traces often observed in metal martensite, were observed(see Fig. 1 or Ref. 10). The striations always appeared nearly parallel to the $(101)_t$ twin traces of the matrix. Thus we assumed that the LIS is either slip or twinning on the $\{101\}_m$ plane which is derived from the $(101)_t$ plane through the LC adopted. On the $\{101\}_m$ plane, $< 10\bar{1} >_m$ and $< 010 >_m$ directions are probable slip directions and $\{101\}_m$ twin is also probable twin system of the m-lattice[12]. Thus these three LIS systems on the $\{101\}_m$ plane are employed in the calculation.

2.5 Orientation relation and habit plane

Lattice orientation relation and habit plane orientation are not necessary for a phenomenological calculation, but they are important for examining the results. The orientation relation in Table 1 was obtained by a precession camera method using a single grain of the t-phase containing many m-plates. Although the c-axis direction of the matrix could not be uniquely identified owing to the presence of three mutually perpendicular t-variants in the herringbone structure, the result clearly showed that the b_m and c_m remained parallel to two of the principal axes of the matrix lattice, while a_m was tilted from the third principal axis. The same orientation relation has been most commonly reported in zirconia systems[2].

A habit plane orientation is usually expressed in terms of Miller indices referred to a parent lattice. When the symmetry of a parent lattice is high, as in the present case(the herringbone structure has a cubic symmetry on an average), it is difficult to uniquely determine the habit plane indices using a single surface trace analysis unless candidates are limited to a small number. On the other hand, since the symmetry of the m-lattice is low, *i.e.* only a mirror reflection across the $(010)_m$ plane, the habit plane could be uniquely determined in the m-basis. The analysis identified the habit plane to be near the $(\bar{3}01)_m$ plane.

3. Procedure of calculation

The phenomenological theory of martensite assumes that a martensite plate forms with an invariant plane strain. This assumption is justified by Eshelby's ellipsoidal inclusion problem[13]. Although a lattice strain itself is not generally an invariant plane strain, an introduction of an appropriate shear by slip or twinning can make the total strain an invariant plane strain.

When the parent lattice is a single variant, the above condition may be expressed by the following matrix equation.

$$\mathbf{S} = \mathbf{RPB} \tag{1}$$

where $\mathbf{B}$ denotes the lattice strain (referred to Bain strain), $\mathbf{P}$ the lattice invariant shear strain, and $\mathbf{R}$ the rigid body rotating. Given $\mathbf{B}$ and the shear system of $\mathbf{P}$, Eq. (1) can be solved. In other words, the matrices $\mathbf{S}$, $\mathbf{R}$, $\mathbf{P}$ can be explicitly determined. Once this is done, the habit plane, the shape strain, orientation relation, *etc.*, can be determined.

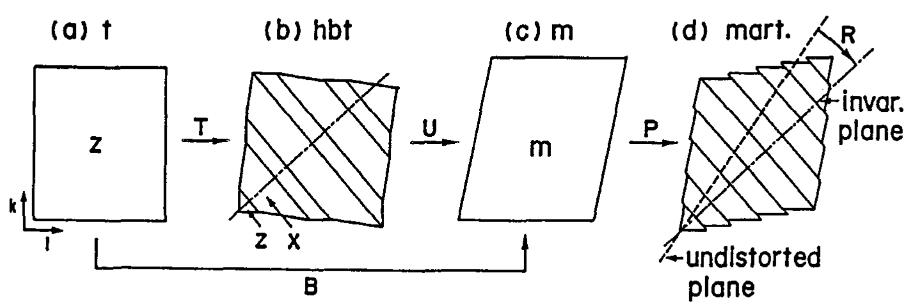

Fig. 3. Diagram showing various stages of the transformation.

In the present case, however, the parent lattice is not a single variant lattice. Instead, it comprises stacks of $(101)_t$ twin layers. A necessary modification of Eq. (1) is described referring to Fig. 3, where (a) denotes the z-variant of the t-lattice, (b) twinned parent lattice, (c) the m-lattice, and in (d) LIS slip is introduced to ensure an undistorted plane (dashed line); a further rotation $\mathbf{R}$ bring the undistorted plane to an invariant plane with respect to the parent lattice (chained line). When the parent lattice is the z-variant, the lattice strain from (a) to (c) can be directly substituted for $\mathbf{B}$ in Eq. (1). While if the parent lattice is the twinned layers, the strain from (b) to (c), *i.e.* $\mathbf{U}$, must be used in place of $\mathbf{B}$ in Eq. (1). Denoting the twinning strain from (a) to (b) by $\mathbf{T}$, the following equations are obvious.

$$\mathbf{B} = \mathbf{UT} \tag{2}$$

and

$$\mathbf{U} = \mathbf{BT}^{-1} \tag{3}$$

A substitution of $\mathbf{U}$ for $\mathbf{B}$ in Eq. (1) yields,

$$\mathbf{S} = \mathbf{RPBT}^{-1} \tag{4}$$

When we choose a twinned band of idealized herringbone structure for structure (b), strain $\mathbf{T}$ is completely known from the twin ratio. Thus, Eq. (4) includes the same number of unknowns as in Eq. (1) and can be solved.

Next, we describe a method of obtaining explicit forms of the matrices $\mathbf{B}$, $\mathbf{T}$, and $\mathbf{P}$. In calculation, it is convenient to describe strain matrices and vectors in an orthonormal coordinate basis. On the other hands, crystallographic parameters are usually referred to the crystal lattice basis. Thus, we first introduce transformation matrices so that we can freely interchange the reference bases. We choose an orthonormal basis parallel to the principal axes of the z-variant and denote the basis by i, while the crystal basis relevant to the z- variant and m-lattice by z and m, respectively. Then, the transformation matrices from z to i basis and m to i basis may be expressed using the lattice parameters, as follow:

$$(i\mathbf{J}z) = \begin{pmatrix} 5.10033 & 0 & 0 \\ 0 & 5.10033 & 0 \\ 0 & 0 & 5.18655 \end{pmatrix} \tag{5}$$

$$(i\mathbf{J}m) = \begin{pmatrix} 5.09887 & 0 & 0 \\ -0.77204 & 0 & 5.32513 \\ 0 & -5.19090 & 0 \end{pmatrix} \tag{6}$$

And the inverse transformation matrices are defined by the corresponding inverse matrices.

$$(z\mathbf{J}i) = (i\mathbf{J}z)^{-1} \tag{7}$$

$$(m\mathbf{J}i) = (i\mathbf{J}m)^{-1} \tag{8}$$

Following Bowles and Mackenzie's notation[4], a vector is transformed by multiplying the column vector to the transformation matrix from the right, while a plane normal is transformed by multiplying the row vector to the inverse transformation matrix form the left. For example, a vector $\mathbf{v}$ and a plane normal $\mathbf{h}$ referred to the z- basis may be converted into the orthonormal basis by the following formulae,

$$[i, \mathbf{v}] = (i\mathbf{J}z)[z, \mathbf{v}] \tag{9}$$

$$(\mathbf{h}, i) = (\mathbf{h}, z)(z\mathbf{J}i) \tag{10}$$

Bain strain referred to the orthonormal basis can be obtained by[4],

$$(i\mathbf{B}i) = (i\mathbf{J}m)(m\mathbf{C}z)(z\mathbf{J}i) \tag{11}$$

where $(m\mathbf{C}z)$ denotes a lattice correspondence matrix. The explicit forms of the above mentioned six lattices correspondences are:

$$\begin{aligned}
(m\mathbf{C}z)^{\mathrm{ABC}} &= \begin{pmatrix} 1 & 0 & 0 \\ 0 & 1 & 0 \\ 0 & 0 & 1 \end{pmatrix} & (m\mathbf{C}z)^{\mathrm{AC\bar{B}}} &= \begin{pmatrix} 1 & 0 & 0 \\ 0 & 0 & -1 \\ 0 & 1 & 0 \end{pmatrix} \\
(m\mathbf{C}z)^{\mathrm{BCA}} &= \begin{pmatrix} 0 & 0 & 1 \\ 1 & 0 & 0 \\ 0 & 1 & 0 \end{pmatrix} & (m\mathbf{C}z)^{\mathrm{\bar{B}AC}} &= \begin{pmatrix} 0 & 1 & 0 \\ -1 & 0 & 0 \\ 0 & 0 & 1 \end{pmatrix} \\
(m\mathbf{C}z)^{\mathrm{CAB}} &= \begin{pmatrix} 0 & 1 & 0 \\ 0 & 0 & 1 \\ 1 & 0 & 0 \end{pmatrix} & (m\mathbf{C}z)^{\mathrm{C\bar{B}A}} &= \begin{pmatrix} 0 & 0 & 1 \\ 0 & -1 & 0 \\ 1 & 0 & 0 \end{pmatrix}
\end{aligned} \tag{12}$$

Slip and twinning are an invariant plane strain, which may be described in terms of the invariant plane normal $\mathbf{p}$ and the shear direction $\mathbf{d}$,

$$\mathbf{P} = \mathbf{I} + m\mathbf{d}\mathbf{p}' \tag{13}$$

where $\mathbf{I}$ denotes a unit matrix and m the amount of shear, $\mathbf{p}'$ denotes the transpose of $\mathbf{p}$. Thus the twinning shear $\mathbf{T}$ from (a) to (b) in Fig. 3 can be calculated from

$$(i\mathbf{T}i) = \mathbf{I} + \frac{2}{3}vg(i\mathbf{J}z)\begin{bmatrix} 1 \\ 0 \\ -1 \end{bmatrix}_z (1 \quad 0 \quad 1)_z\,(z\mathbf{J}i) \tag{14}$$

where g is the factor which normalizes the vectors $(101)_z(z\mathbf{J}i)$ and $(i\mathbf{J}z)[10\bar{1}]_z$ represented in the orthonormal basis. v is the amount of shear for a complete twinning ($v = (c^2 - a^2)/a = 0.0354$). Since the structure in Fig. 3(b) comprises twins of the x and z variants with a ration 2, T is 2/3 of complete twinning.

When the LIS is slip, the LIS matrix can be calculated in the similar way from the slip plane and direction. The plane was assumed to be the $\{101\}_m$ plane which corresponds to the $(101)_z$ plane. Thus the explicit indices varies depending on the lattice correspondence adopted. In case of $AC\bar{B}$ lattice correspondence, for example, the slip plane in the m-lattice is

$$(1 \quad 0 \quad 1)_z\,(z\mathbf{C}m)^{\mathrm{AC\bar{B}}} = (1 \quad 0 \quad 1)_z \begin{pmatrix} 1 & 0 & 0 \\ 0 & 0 & 1 \\ 0 & -1 & 0 \end{pmatrix} = (1 \quad -1 \quad 0)_z \tag{15}$$

Thus, the slip direction is $[110]_m$ or $[001]_m$, since we consider two types of shear directions namely $< 10\bar{1} >_m$ and $< 010 >_m$. For the former case, the LIS strain is expressed by:

$$\begin{aligned} (i\mathbf{P}i) &= \mathbf{I} + th(i\mathbf{J}m)\begin{bmatrix} 1 \\ 1 \\ 0 \end{bmatrix}_m (1 \quad -1 \quad 0)_m\,(m\mathbf{J}i) \\ &= \mathbf{I} + t\begin{pmatrix} -0.49713 & 0.0 & -0.48832 \\ 0.07527 & 0.0 & 0.07394 \\ 0.50610 & 0.0 & 0.49713 \end{pmatrix}_i \end{aligned} \tag{16}$$

where h is the normalization factor for the two succeeding vectors in the orthonormal basis, t denote the amount of shear.

For the twinning LIS, the shear direction must be first determined. Taking the same LC as above, for example, the twinning plane in the m-lattice is $(1\bar{1}0)_m$. Then the twinning elements K_1 and η_2 are $(1\bar{1}0)_m$ and $[1\bar{1}0]_m$, respectively. Referring to Fig. 4, the shear direction $\mathbf{d}$ and the amount of shear s are calculated using the following equations.

$$\begin{aligned} K_1 &= (1 \quad -1 \quad 0)_m\,(m\mathbf{J}i) \\ \eta_2 &= (i\mathbf{J}m)\begin{bmatrix} 1 \\ -1 \\ 0 \end{bmatrix}_m \\ s &= 2\tan(\cos^{-1}(\overline{K}_1 \cdot \overline{\eta}_2)) \\ \mathbf{d} &// (\overline{K}_1 \cdot \overline{\eta}_2)\overline{K}_1 - \overline{\eta}_2 \\ \bar{\mathbf{d}} &= \mathbf{d}/\ \mid \mathbf{d} \mid \end{aligned} \tag{17}$$

where the attached bars denote unit vectors along the corresponding vectors. Using shear plane normal $\overline{K}_1$ and shear direction $\bar{\mathbf{d}}$, the twin strain is expressed by

$$\begin{aligned} (i\mathbf{P}i) &= fs\bar{\mathbf{d}}\overline{K}'_1 \\ &= \mathbf{I} + t\begin{pmatrix} 0.08310 & 0.0 & 0.08163 \\ 0.70348 & 0.0 & 0.69101 \\ -0.08460 & 0.0 & -0.08310 \end{pmatrix} \end{aligned} \tag{18}$$

where f denotes a twin fraction, thus fs describes the amount of shear t. Both Eqs. (16) and (18) include an amount of shear t as a parameter.

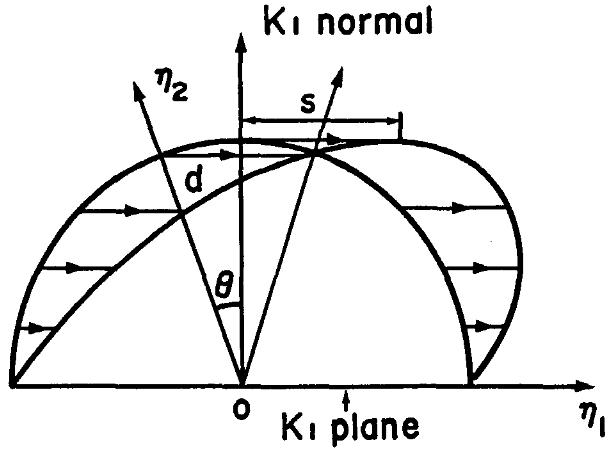

Fig. 4. Diagram showing the geometry of a twin deformation. K_1, η_1, and η_2 are the usual twin elements. d and s denote the direction and amount of shear.

Including the above calculations, calculations to solve Eq. (4) and the subsequent calculations of physical parameters, such as habit plane, orientation relation, *etc.*, from the solution are carried out through a computer program. Equation (4) is solved through the following three steps.

First, $\mathbf{R}$ in Eq. (4) is eliminated by multiplying its transpose.

$$\begin{aligned} \mathbf{S'S} &= (\mathbf{RPBT}^{-1})'(\mathbf{RPBT}^{-1}) \\ &= (\mathbf{PBT}^{-1})'(\mathbf{R'R})(\mathbf{PBT}^{-1}) \\ &= (\mathbf{PBT}^{-1})'(\mathbf{PBT}^{-1}) \end{aligned} \tag{19}$$

The above equation contains only one parameter, t. The condition that $\mathbf{S}$ is an invariant plane strain is equivalent to that one of the eigen values of Eq. (19) is unity and the remaining two are smaller and greater than unity, respectively. A critical value of t, *i.e.* t_c, which fulfills this condition is numerically sought.

Then, t_c is substituted into Eq. (4), and which follows:

$$\mathbf{R'S} = \mathbf{PBT}^{-1} \tag{20}$$

The strain described by Eq. (20) contains generally two undistorted planes. The eigenvector corresponding to the unit eigenvalue lies on the undistorted planes. Two other undistorted vectors normal to the unit eigenvector can be determined from the ratio of the other two eigenvalues. The combination of these two undistorted vectors with the unit eigenvector defines two undistorted planes.

Finally $\mathbf{R}$ is determined so that one of the undistorted plane is brought back to the initial orientation so that the plane become invariant (undistorted and unrotated).

In this way, all the matrices in Eq. (4) are explicitly determined. It is a simple matter to find the invariant plane, orientation relations, the total shape distortions, *etc.*, in the orthonormal basis and convert them into either of the crystal bases.

4. Results and Discussion

Table 2 shows the number of solutions for the critical shear which ensures the middle eigenvalue of Eq. (19) becomes unity for each combination of the three LIS systems with the six LCs. Among the eighteen combinations eight yield one or two t_c's. For each t_c, since there exist a pair of undistorted planes, two solutions conjugate each other result depending on which of the undistorted planes is selected to be invariant. All the solutions are listed in Table 3(a)-(c) separately for the three types of LIS systems.

Tabel 2. Number of solutions of the critical values of LIS

		LIS system		
LC No.	LC	$\{101\} < 10\bar{1} >_m$	$\{101\} < 010 >_m$	$\{101\}_m$ twin
1	ABC	0	0	0
2	$AC\bar{B}$	1	1	2
3	BCA	1	1	2
4	$\bar{B}AC$	1	0	0
5	CAB	1	0	0
6	$C\bar{B}A$	0	0	0

Table 3.(a) Solutions for LIS = $\{101\} < 10\bar{1} >_m$ slip

Parameter	Solution			
LC	2 $AC\bar{B}$	3 BCA	4 $\bar{B}AC$	5 CAB
LIS	$(1\bar{1}0)[110]_m$	$(110)[1\bar{1}0]_m$	$(0\bar{1}1)[011]_m$	$(011)[01\bar{1}]_m$
t_c	0.02416	0.01293	0.01293	-0.02417
m	0.15763	0.15763	0.15799	0.15799
$\mathbf{h}_1$	(0.96011, -0.27962, 0.00085)	(-0.01694, 0.27962, -0.95996)	(-0.00482, 0.95867, -0.28449)	(-0.28453, 0.95867, 0.00005)
$\mathbf{d}_1$	[0.00381, -0.99999, -0.00020]	[0.00014, 0.99999, -0.00381]	[-0.01761, -0.00197, -0.99984]	[-1.00000, -0.00197, -0.00085]
$[100]_t\wedge$	$[100]_m$ 8.60°	$[010]_m$ 1.01°	$[0\bar{1}0]_m$ 1.01°	$[001]_m$ 0.05°
$[010]_t\wedge$	$[001]_m$ 0.01°	$[001]_m$ 0.01°	$[100]_m$ 8.62°	$[100]_m$ 8.62°
$[001]_t\wedge$	$[0\bar{1}0]_m$ 0.05°	$[100]_m$ 8.66°	$[001]_m$ 1.01°	$[010]_m$ 0.05°
$\mathbf{h}_2$	(0.07753, -0.99699, -0.00013)	(-0.00117, 0.99699, -0.07752)	(-0.01755, 0.07194, -0.99725)	(-0.99741, 0.07194, -0.00084)
$\mathbf{d}_2$	[0.97811, -0.20807, 0.00088]	[-0.01727, 0.20807, -0.97796]	[-0.00355, 0.97708, -0.21286]	[-0.21289, 0.97708, 0.00002]
$[100]_t\wedge$	$[100]_m$ 0.15°	$[010]_m$ 1.01°	$[0\bar{1}0]_m$ 1.01°	$[001]_m$ 8.47°
$[010]_t\wedge$	$[001]_m$ 8.47°	$[001]_m$ 8.47°	$[100]_m$ 0.14°	$[100]_m$ 0.14°
$[001]_t\wedge$	$[0\bar{1}0]_m$ 0.05°	$[100]_m$ 1.02°	$[001]_m$ 8.53°	$[010]_m$ 0.05°

We now examine these results. In all solutions the amount of LIS shear(t_c), and the amount of shape strain (m) are less than 0.2 and appear to be reasonably small. Orientation relations are described in terms of angles between the corresponding principal axes of the two lattices. They can be grouped into three types, namely (i) b_m and c_m remain parallel to the principal axes of the parent lattice, while a_m is inclined, (ii) a_m and b_m remain parallel to the principal axes of the parent lattice, while c_m is inclined, (iii) all of the m-axes are inclined several degrees from the principal axes of the parent lattice. One of the conjugate solutions (listed in the upper case in Table 3(a)-(c)) are of type (i), while the others (lower case) are either of type (ii) or (iii). Thus, only those solutions in the upper case in Table 3(a)-(c) agree with the observed orientation relation (see Table 1).

We next examine the habit planes of the ten solutions which agree with the experimental orientation relation. Since the habit planes in Table 3(a)-(c) are described in reference to the

Table 3.(b) Solutions for LIS = $\{101\}$ $< 010 >_m$ slip

Parameter	Solution	
LC	2 $AC\bar{B}$	3 BCA
LIS	$(1\bar{1}0)[001]_m$	$(110)[001]_m$
t_c	0.11795	0.11489
m	0.11775	0.11566
$\mathbf{h}_1$	(0.63073, -0.38379, -0.67445)	(0.66620, 0.38376, -0.63946)
$\mathbf{d}_1$	[-0.16072, -0.97424, -0.15819]	[0.08720, 0.99274, 0.08286]
$[100]_t\wedge$	$[100]_m$ 9.10°	$[010]_m$ 0.36°
$[010]_t\wedge$	$[001]_m$ 0.56°	$[001]_m$ 0.29°
$[001]_t\wedge$	$[0\bar{1}0]_m$ 1.37°	$[100]_m$ 8.82°
$\mathbf{h}_2$	(-0.12072, -0.97368, -0.19330)	(0.12281, 0.99142, 0.04482)
$\mathbf{d}_2$	[0.65283, -0.33559, -0.67911]	[0.67490, 0.33552, -0.65721]
$[100]_t\wedge$	$[100]_m$ 4.50°	$[010]_m$ 4.40°
$[010]_t\wedge$	$[001]_m$ 5.94°	$[001]_m$ 5.94°
$[001]_t\wedge$	$[0\bar{1}0]_m$ 4.28°	$[100]_m$ 4.55°

Table 3.(c) Solutions for LIS = $\{101\}_m$ twin

Parameter	Solution			
LC	2 AC$\bar{B}$-1	2 AC$\bar{B}$-2	3 BCA-1	3 BCA-2
LIS	$(1\bar{1}0)_m$ twin	$(1\bar{1}0)_m$ twin	$(110)_m$ twin	$(110)_m$ twin
t_c	0.11587	0.13440	0.08084	0.09937
m	0.11512	0.11785	0.11785	0.11512
$\mathbf{h}_1$	(-0.60293, 0.38318, 0.69974)	(-0.47005, 0.37401, 0.79948)	(0.47005, 0.37401, -0.79948)	(0.60293, 0.38318, -0.69974)
$\mathbf{d}_1$	[0.02756, 0.99914, 0.03092]	[0.00551, 0.99994, 0.00936]	[-0.00551, 0.99994, -0.00936]	[-0.02756, 0.99914, -0.03092]
$[100]_t\wedge$	$[100]_m$ 8.68°	$[100]_m$ 8.62°	$[010]_m$ 1.05°	$[010]_m$ 1.24°
$[010]_t\wedge$	$[001]_m$ 0.10°	$[001]_m$ 0.03°	$[001]_m$ 0.03°	$[001]_m$ 0.10°
$[001]_t\wedge$	$[0\bar{1}0]_m$ 0.22°	$[0\bar{1}0]_m$ 0.04°	$[100]_m$ 8.65°	$[100]_m$ 8.62°
$\mathbf{h}_2$	(-0.00698, 0.99755, 0.06955)	(-0.02167, 0.99824, 0.05516)	(0.02167, 0.99824, -0.05516)	(0.00698, 0.99755, -0.06955)
$\mathbf{d}_2$	[-0.61682, 0.33485, 0.71233]	[-0.47996, 0.32408, 0.81524]	[0.47996, 0.32408, -0.81524]	[0.61682, 0.33485 -0.71233]
$[100]_t\wedge$	$[100]_m$ 4.72°	$[100]_m$ 5.51°	$[010]_m$ 3.30°	$[010]_m$ 4.06°
$[010]_t\wedge$	$[001]_m$ 5.95°	$[001]_m$ 6.12°	$[001]_m$ 6.12°	$[001]_m$ 5.95°
$[001]_t\wedge$	$[0\bar{1}0]_m$ 4.50°	$[0\bar{1}0]_m$ 5.27°	$[100]_m$ 3.45°	$[100]_m$ 4.20°

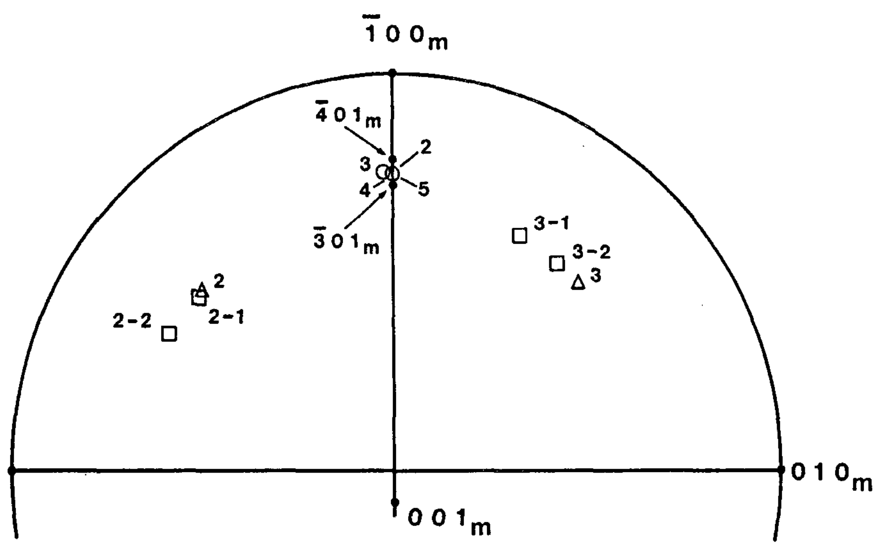

Fig. 5. Predicted habit planes for various LIS systems, ○ :$\{101\} < 10\bar{1} >_m$, △ :$\{101\}$ $< 010 >_m$, □ :$\{101\}_m$ twin

orthonormal basis, they are converted to the m-lattice basis to allow a direct comparison with the observed habit plane orientation. These are projected on a stereograph of the m-lattice in Fig. 5. The habit plane of a particular solution may be identified in the plot by the LIS type and LC number. It is seen that all four solutions for the $\{101\} < 10\bar{1} >_m$ LIS system results in approximately the same habit plane near $(\bar{3}01)_m$, whereas those for the other two LIS systems result in distinctly different orientations. Since experimental habit plane is close to $(\bar{3}01)_m$, only those solutions with $\{101\} < 10\bar{1} >_m$ LIS system agree with observation.

Since these four solutions are not crystallographically equivalent, a further examination was

Tabel 4. Number of solutions of the critical values of LIS(Single variant parent lattice)

LC Code	LC	LIS system 1 $(110)[1\bar{1}0]_m$	2 $(011)[0\bar{1}1]_m$	3 $(101)[\bar{1}01]_m$	4 $(10\bar{1})[101]_m$
C	ABC	1	1[*4]	0	0
A	BCA	1[*3]	1	0	0
B	CAB	1[*2]	1[*5]	0	0

*2~*5 correspond to the solutions 2~5 in Table 3(a), respectively.

Table 5. Solutions for LIS = $\{101\} < 10\bar{1} >_m$ slip (Single variant parent lattice)

Parameter	Solution					
LC	ABC-1	ABC-2[*4]	BCA-1[*3]	BCA-2	CAB-1[*2]	CAB-2[*5]
LIS	$(110)[1\bar{1}0]_m$	$(011)[0\bar{1}1]_m$	$(110)[1\bar{1}0]_m$	$(011)[0\bar{1}1]_m$	$(110)[1\bar{1}0]_m$	$(011)[0\bar{1}1]_m$
t_c	0.03542	0.03541	0.03504	0.35418	0.00169	0.00169
m	0.15434	0.15799	0.15763	0.16876	0.15763	0.15799
h_1	(-0.98453,	(0.95867,	(-0.01694,	(0.00293,	(-0.27962,	(-0.28453,
	-0.01777,	-0.00482,	0.27962,	0.37334,	0.96011,	0.95867,
	0.17431)	-0.28449)	-0.95996)	-0.92769)	0.00085)	-0.00005)
d_1	[-0.11809,	[-0.00197,	[0.00014,	[0.01734,	[-0.99999,	[-1.00000,
	0.00224,	-0.01761,	0.99999,	0.99326,	0.00381,	-0.00197,
	0.99300]	-0.99984]	-0.00381]	0.11458]	-0.00020]	-0.00085]
$[100]_t\wedge$	$[100]_m$ 8.49°	$[100]_m$ 8.62°	$[010]_m$ 1.01°	$[010]_m$ 1.03°	$[001]_m$ 0.01°	$[001]_m$ 0.05°
$[010]_t\wedge$	$[010]_m$ 0.99°	$[010]_m$ 1.01°	$[001]_m$ 0.01°	$[001]_m$ 1.10°	$[100]_m$ 8.60°	$[100]_m$ 8.62°
$[001]_t\wedge$	$[001]_m$ 0.18°	$[001]_m$ 1.01°	$[100]_m$ 8.66°	$[100]_m$ 9.00°	$[010]_m$ 0.05°	$[010]_m$ 0.05°
h_2	(-0.18934,	(0.07194,	(-0.00117,	(0.01715,	(-0.99699,	(-0.99741,
	0.00085,	-0.01755,	0.99699,	0.99923,	0.07753,	0.07194,
	0.98191)	-0.99725)	-0.07752)	0.03540)	-0.00013)	-0.00084)
d_2	[-0.99452,	[0.97708,	[-0.01727,	[0.00155,	[-0.20807,	[-0.21289,
	-0.01827,	-0.00355,	0.20807,	0.29857,	0.97811,	0.97708,
	0.10289]	-0.21286]	-0.97796]	-0.95439]	0.00088]	0.00002]
$[100]_t\wedge$	$[100]_m$ 1.04°	$[100]_m$ 0.14°	$[010]_m$ 1.01°	$[010]_m$ 0.99°	$[001]_m$ 8.47°	$[001]_m$ 8.47°
$[010]_t\wedge$	$[010]_m$ 1.03°	$[010]_m$ 1.01°	$[001]_m$ 8.47°	$[001]_m$ 8.77°	$[100]_m$ 0.15°	$[100]_m$ 0.14°
$[001]_t\wedge$	$[001]_m$ 8.44°	$[001]_m$ 8.53°	$[100]_m$ 1.02°	$[100]_m$ 0.10°	$[010]_m$ 0.05°	$[010]_m$ 0.05°

*2~*5 see the footnote of Table 4.

made to see if all of these appear in practice. Recasting of the predicted habit planes onto the t-basis stereograph enabled to distinguish each of the solution from others. The habit plane traces of five observed plates in a single twin band passed all four predicted habit plane normals and this fact indicated that all of the four solutions indeed exist[11].

So far all the calculations were made for a particular band with the twin ratio of 2. In practice, the twin ratio varies from one place to another. For a twin band with an arbitrary twin ratio, solutions could be obtained by substituting an appropriate twin ratio in place of the factor 2/3 of the second term on the right hand side of Eq. (14). However, it was proved that a variation of the twin ratio does not change the result except for the amount of LIS[11]. This fact arises from the equivalence of the $(101)_t$ twin in the parent lattice and the slip on the corresponding $\{101\}_m$ plane along the $< 10\bar{1} >_m$ direction. Thus a change in the twin ratio in the parent is compensated by an appropriate amount of the slip in the m-lattice. This may be understood by the fact that in the phenomenological theory, LIS is often employed in the parent lattice instead of the martensite without altering the result.

Next we consider the case where the parent lattice is a single variant t-phase. A substitution of zero into the twin ratio of Eq. (14) makes the equation applicable to such a case. But from the above argument, as long as the same LIS system is assumed, the same solutions as before are expected to arise. However, for a twinned band, the plane of LIS was selected to be the $\{101\}_m$ plane which was derived from the $(101)_t$ plane through the lattice correspondence. Thus if there are no twins, any of the six $\{101\} < 10\bar{1} >_m$ slip systems are equally probable. (Among these six planes, $(110)_m$ and $(1\bar{1}0)_m$, and $(011)_m$ and $(0\bar{1}1)_m$ are crystallographically equivalent. Thus, there arise four non-equivalent LIS systems.) On the other hand, for a single z-variant, since a and b axes are equivalent, only three nonequivalent LCs arise, namely ABC, BCA, and CAB. For all the

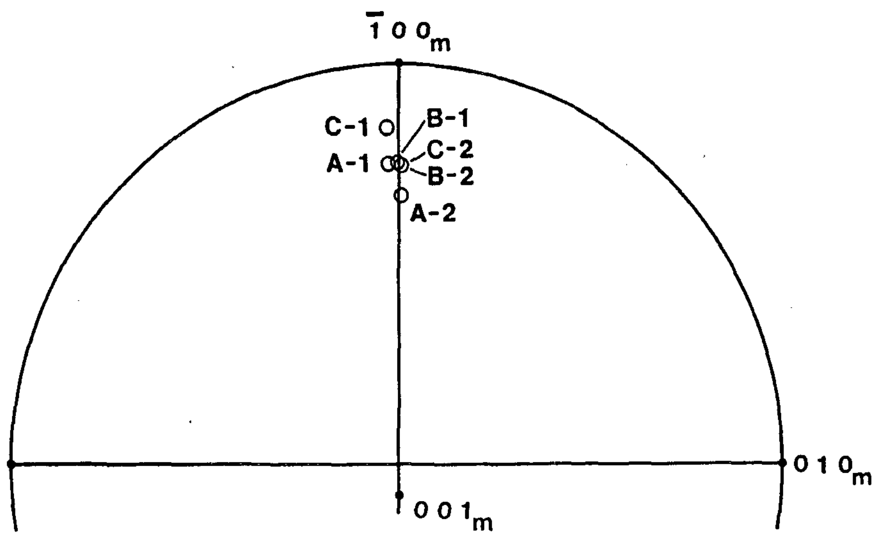

Fig. 6. Predicted habit planes for a single variant parent lattice. $\{101\} < 10\bar{1} >_m$ slip is assumed for LIS.

combinations of the four LISs and the three LCs, similar calculations were conducted as before.

Table 4 lists the number of critical LIS resulting in a unit eigenvalue. Recalling that the lattice correspondences $AC\bar{B}$ and $\bar{B}AC$ are equivalent to CAB and ABC, respectively, for a single variant t-lattice, it is seen that four of the six LC-LIS combinations with a solution are the same as listed in the third column of Table 2. As explained previously, these four combinations result in the same as those in Table 3(a) except for the t_c values (see Table 5). Thus, for a single variant t-lattice, only two extra pairs of solutions arise, in which only one of the conjugate solutions satisfies the observed orientation relation as before. The habit planes of all six solutions listed in Table 5 are plotted in Fig. 6. The symbols denote the combination of the LC code and LIS number in Tables 4 and 5. The habit plane of the new solutions are $(\bar{11}02)_m$ and $(\bar{5}02)_m$, which are 6 deg apart from the previously obtained $(\bar{7}02)_m$ in the opposite directions. An experimental distinction among the three habit plane orientations requires a careful trace analysis.

Lee *et al.*[14] reported $(401)_t$ and $(410)_t$ habit planes for m-plates formed in a single variant t-grain. The presently predicted habit planes indices in the m- lattice basis change little when they are converted into the t-lattice basis, apart from the order of indices which depends on the LC adopted. Thus, the present habit planes may be expressed by $\{702\}_t$, $\{1102\}_t$ and $\{502\}_t$. The habit planes reported by Lee *et al.* are quite close to the presently predicted $\{702\}_t$ plane.

Finally the influence of the lattice parameter deviations, which may arise from experimental error or variation of the alloy composition, on the result is briefly examined. Calculations were made for two cases, one with $c/a = 1.013$ keeping the unit cell volume constant and the other with the lattice parameters 0.5% greater keeping $c/a = 1.017$. In the former case the habit plane deviated by $0.5°$, while in the latter by $2°$. The influence to the lattice orientation were even smaller; in both cases about $0.2°$. These deviations were smaller than the usual experimental error and thus the deviation of the lattice parameters of the order considered here is unlikely to alter the conclusions of the present analysis.

5. Summary

The phenomenological theory was applied ton the herringbone tetragonal to thin plate monoclinic transformation in an arc-melted ZrO_2- 2mol%Y_2O_3 alloy. Comparisons of the calculated results and observedat a in habit planes and orientation relations lead to the following conclusions.

1. The LIS is likely to be the slip in the $\{101\} < 10\bar{1} >_m$ system on the plane which corresponds to the $(101)_t$ twin plane of the parent lattice.
2. Corresponding to four different LCs, four different solutions result, but they are all similar and assume a $(\bar{7}02)_m$ habit plane.
3. When the parent lattice is a single variant tetragonal lattice, i.e. free from twins, two extra solutions are predicted, in addition to the above four. Their habit planes are $(\overline{11}02)_m$ and $(\bar{5}02)_m$.

References

1) G. M. Wolten: "Diffusionless Phase Transformations in Zirconia and Hafnia", *J. Amer. Ceram. Soc.*, **46** [9] 418-422 (1963)
2) G. K. Bansal and A. H. Heuer: "On a Martensitic Phase Transformation in Zirconia (ZrO_2) —I. Metallographic Evidence", *Acta metall.*, **20** [11] 1281-89 (1972)
3) M. S. Wechsler, D. S. Lieberman and T. A. Read: "On the Theory of the Formation of Martensite", *Trans. Am. Inst. Min. Engrs.*, **197** [11] 1503-15 (1953)
4) J. S. Bowles and J. K. Mackenzie: "The Crystallography of Martensite Transformations I", *Acta metall.*, **2** [1] 129-37 (1954), "The Crystalloraphy of Martensite Transformations II", *ibid.*, **2** [1] 138-47 (1954)
5) G. K. Bansal and A. H. Heuer: "On a Martensitic Phase Transformation in Zirconia (ZrO_2) —II. Crystallographic Aspects", *Acta metall.*,**22** [4] 409-17 (1974)
6) W. M. Kriven, W. L. Fraser and S. W. Kennedy: "The Martensite Crystallography of Tetragonal Zirconia", pp.82-97 in Advances in Ceramics, Vol.3, Science and Technology of Zirconia, Edited by A. H. Heuer and L. W. Hobbs, American Ceramic Society, Columbus, Ohio (1981)
7) M. A. Choudhry and A. G. Crocker: "Theory of Twinning and Transformation Modes in Zirconia", pp.46-53 in Advances in Ceramics, Vol.12, Science and Technology of Zirconia II, Edited by N.Claussen, M. Rühle and A. H. Heuer, American Ceramic Society, Columbus, Ohio (1984)
8) P. M. Kelly and C. J. Ball: "Crystallography of Stress-Induced Martensitic Transformations in Partially Stabilized Zirconia", *J. Am. Ceram. Soc.*, **69** [3] 259-64 (1986)
9) M. Hayakawa, M. Tada, H. Okamoto and M. Oka: "Structural Study on the Cubic to Tetragonal Transformation in Arc-melted ZrO_2-3mol%Y_2O_3", *Trans. Japan Inst. Metals*, **27** [10] 750-60 (1986)
10) M. Hayakawa, N. Kuntani and M. Oka: "Structural Study on the Tetragonal to Monoclinic Transformation in Arc-melted ZrO_2-2mol%Y_2O_3 —I. Experimental Observations", *Acta metall.*, **37** [8] 2223-28 (1989)
11) M. Hayakawa and M. Oka: "Structural Study on the Tetragonal to Monoclinic Transformation in Arc-melted ZrO_2-2mol%Y_2O_3 —II. Quantitative Analysis", *Acta metall.*, **37** [8] 2229-35 (1989)
12) J. E. Bailey: "The Monoclinic-Tetragonal Transformation and Associated Twinning in Thin Films of Zirconia", *Proc. Roy. Soc.* A, **279** 395-412 (1964)
13) J. D. Eshelby: "The Determination of the Elastic Field of an Ellipsoidal Inclusion, and Related Problems", *Proc. Roy. Soc.* A, **241** 376-96 (1957)
14) R.-R. Lee and A. H. Heuer: "*In Situ* Martensitic Transformation in a Ternary $MgO-Y_2O_3-ZrO_2$ Alloy: I, Transformation in Tetragonal ZrO_2 Grains", *J. Am. Ceram. Soc.*, **71** [8] 694-700 (1988)